USING OPTICAL SATELLITE IMAGES AND SATELLITE ALTIMETRY DATA TO ESTIMATE VOLUME VARIATIONS IN DAMS

R. Ghanbari[1], A. Tayfehrostami[2*], M. Forouzanfar[3], M. Tashakori[4]

[1] Department of Computer Science, University of Iowa, Iowa 52242, USA – (ronak-ghanbari@uiowa.edu)
[2] Faculty of Geodesy and Geomatics Engineering, K. N. Toosi University of Technology, Tehran 1996715433, Iran – (a.tayfehrostami@email.kntu.ac.ir)
[3] Master of Remote Sensing & GIS, University of Research Sciences, Tehran, Iran – (M.forouzanfar1985@gmail.com)
[4] Technical Expert, Water and Wastewater company, Bandar-e Anzali, Gilan, Iran – (tashakorisurvey@gmail.com)

KEY WORDS: Volume Variations, Dams, Satellite Altimetry, Satellite Imagery, Water Level, Water Surface Area.

ABSTRACT:

This study focused on monitoring the water volume variations of the Doroudzan dam reservoir in Shiraz, Iran, using satellite observations. In particular, Sentinel-3 altimetry mission (SRAL) Level-1B and Level-2 data were employed to calculate water level changes, addressing the limitations in accuracy for inland and shallow waters. Re-tracking of returned waveforms was applied to improve the accuracy of Level-2 altimetry results. Additionally, Sentinel-2 optical images were utilized to monitor the water surface area of the dam reservoir. The results demonstrated that re-tracking the returned waveforms significantly improved the water level observations compared to Level-2 data. The analysis extended to comparing the time series of water surface area estimated from Sentinel-2 images with in-situ data, revealing a high accuracy of 5.39%. Combining optimum water level and surface area data in Heron's equation facilitated the calculation of water volume variations. A remarkable correlation of 95.27% was found when comparing the time series of estimated water volume variations and in-situ data. This study underscores the effectiveness of Copernicus satellites, particularly Sentinel-3 and Sentinel-2 missions, in monitoring inland water bodies and demonstrates the reliability of the techniques employed for tracking dam reservoir volume variations.

1. INTRODUCTION

Water stands as the most precious resource in nature. Given the escalating expenses associated with establishing sustainable, freshwater sources, it emerges as one of the foremost concerns across all human societies (Kim et al., 2008). The total water volume on Earth is estimated to be approximately 333 million cubic kilometres. This comprises 97.5% saltwater and 2.5% freshwater, with a mere 0.3% of the latter existing in a liquid state on Earth's surface, encompassing lakes, dams, and rivers (Eakins & Sharman, 2010; Gleick, 19993). Dams and reservoirs play a pivotal role in social and economic development. These reservoirs serve various purposes, such as the generation of electric energy, mitigation of floods, and provision of water resources for human consumption, industrial use, and irrigation (Nilsson, 2009; W. Wang et al., 2017; Zarfl et al., 2015; Zhou et al., 2016). The critical parameter in monitoring dam reservoirs is the volume of water stored, a factor directly influenced by the water level (J. F. Crétaux et al., 2016).

Satellite altimetry missions were initially conceptualized and organized for ocean monitoring, typically focusing on studying glaciers and sea ice. Despite the continuous recording of data worldwide by altimetry satellites, no specific mission has been tailored for monitoring inland water bodies. The Brown re-tracker, designed for inland water bodies with highly variable returned waveforms, is available but inefficient. Consequently, various re-tracking methods have been developed to measure rivers, lakes, reservoirs, and wetlands (Tarpanelli & Benveniste, 2019). In the initial studies on inland water bodies, the monitoring of water levels in the Great Lakes in the United States and Africa was conducted using altimetry data from Seasat, Geosat, and TOPEX/Poseidon satellites (Birkett, 1995; Cazenave et al., 1997; Mercier et al., 2002; Morris & Gill, 1994). Subsequent research expanded the application of altimetry to rivers, including the Amazon, Negro, Ob, Mekong, Ganges, Brahmaputra, and Po, among others (Birkinshaw et al., 2010; Domeneghetti et al., 2014; Frappart, Calmant, et al., 2006; Kouraev et al., 2004; Leon et al., 2006; Tarpanelli et al., 2013).

Due to the large footprint of the satellite, which exceeds the width of water in small to medium rivers (ranging from 40 to 800 meters), the topography around the river introduces noise into the radar's return signal. Consequently, water level measurement is more effective for wide rivers than narrow ones. However, this also depends on the type of altimetry sensor available on the satellite (LRM or SAR). For instance, in the Amazon River, the world's largest river, Santos da Silva et al., (2010) achieved an RMSE of about 30 cm with the Envisat satellite. With SAR altimeters, accuracy improves, enabling the monitoring of narrower rivers due to their high resolution along the track (Schneider et al., 2018).

However, processing satellite altimetry measurements for small to medium rivers is intricate due to the large footprint of the antenna, even in cross-direction SAR mode (which has the same footprint width as conventional altimetry). Unique re-tracking algorithms have been developed to estimate water level changes precisely and process complex reflection waves (Biancamaria et al., 2017; Sulistioadi et al., 2015).

Recently, the combination of satellite radar altimetry with satellite images has been employed to assess changes in water volume in large river basins, such as the Negro River basin (Frappart et al., 2005, 2008, 2011), the downstream basin of the Mekong River (Frappart, Do Minh, et al., 2006), and the lower Ob River basin (Frappart et al., 2010). Several studies have

* Corresponding author

attempted to analyze changes in water volume for lakes and reservoirs of dams using the integrated approach of satellite altimetry data and satellite images.

The changes in the volume of the Aral Lake were reconstructed utilizing a digital bathymetry model and water level data obtained from the TOPEX/Poseidon (T/P) altimetry mission (J.-F. Crétaux et al., 2005). A separate study established the relationship between water level and water volume for the Fengmen Dam reservoir using water level data from in-situ gauges and water surface area data obtained from Landsat mission images (Peng et al., 2006). Another study focused on Dongying Lake, China, converted the water level data from the T/P altimetry mission to water storage using the established relationship between water level and water storage, derived from T/P altimetry data and in-situ water storage measurements (Zhang et al., 2006). The water storage changes in nine lakes of the Peace-Athabasca Delta in Canada were calculated using water level data from in-situ gauges and water surface area data from remote sensing images (Smith & Pavelsky, 2009). Additionally, changes in the water volume of Lake Isabel were analyzed using the Heron method's approximate relationship. This analysis utilized altimetry data from the Envisat mission (RA-2) obtained through the Ice-1 re-tracking algorithm, in-situ gauges, and water surface area data obtained from Envisat radar images (ASAR) processing. The study covered the period between February 2003 and December 2006 (Medina et al., 2010).

The methods mentioned above rely on the availability of bathymetric maps, in-situ gauges, or water volumes, which can be challenging or impossible for most remote lakes. Recently, a combination of GRACE satellite gravity measurements with satellite altimetry and optical satellite imagery data has been employed to investigate water volume variations in large inland waters, as seen in the study on the Aral Sea (Singh et al., 2012). However, the characteristics of GRACE impose limitations on its meaningful application to study areas smaller than 200,000 square kilometres. This constraint is a significant drawback for hydrological studies involving many lakes and dam reservoirs with relatively small sizes (Singh et al., 2012). In another study, the volume of Lake Mead in the United States of America and Lake Tana in Ethiopia was compared based on the lowest water level values using GRLM, RLH, Hydroweb, ICESat-GLAS, and water surface area data from satellite images. The water surface resulting from the processing of Landsat TM/ETM+ images was examined using the surface-height relationship integration method (Duan & Bastiaanssen, 2013). In monitoring the water volume variations of Lake Victoria, elevation data from ERS-1, ERS-2, and Envisat obtained through the Ice-1 re-tracking algorithm, along with water surface area data from MODIS/Terra image processing, were used over 22 years (Tong et al., 2016). Also, in Iran, some studies have been related to the watersheds, as described in the sources (Ahmadi et al., 2022; Barezaei & Jalali, 2023; He et al., 2023; Jalali et al., 2021; Kordi & Yousefi, 2022; Mohammadpouri et al., 2023).

Another study focused on the vital role of monitoring lake dynamics in understanding water balance, resource management, and ecological sustainability. Concentrating on Lake Victoria, Africa's largest lake, the research utilizes 15 years of multi-source satellite data, including MODIS, Jason-1/-2/-3, and GRACE, to estimate water volume changes. The methodology involves deriving water level and surface area data from satellite altimetry and imagery, constructing accurate regression models, and comparing results with terrestrial water storage changes from GRACE data. The findings reveal consistent trends in water volume changes and terrestrial water storage. Multi-timescale analyses, encompassing inter-annual, inter-monthly, and variation periods, provide comprehensive insights into Lake Victoria's dynamic water volume fluctuations (Lin et al., 2020). Recently, a study utilized ICESat-2 and Google Earth Engine to monitor water level and volume changes in 11 lakes and eight reservoirs within the Yellow River Basin. In-situ validation demonstrates a low Root Mean Square Error of 7 cm. Seasonal variations are noted in natural lake water levels, while reservoirs exhibit sharp rises and falls. Precipitation significantly influences natural lake levels and indirectly impacts reservoir water discharges. The research indicates that uncertainty in water volume change estimation using ICESat-2 and GEE is less than 9% (Liu et al., 2022). Also, A different study estimated the monthly variation in surface water volume in the Thac Mo hydroelectric reservoir, located in South Vietnam, from 2016 to 2021. By utilizing Sentinel-1 observations for surface water extent and Jason-3 altimetry data for water level variation, the study reveals that, except for the drought years in 2019 and 2020, the surface water extent of the Thac Mo reservoir varies from 50 to 100 km², and the water level ranges from 202 to 217 meters. High correlations are observed between surface water extent and level ($R = 0.948$), Sentinel-1 and Sentinel-2 observations ($R = 0.98$), and Jason-3 altimetry data and in situ measurements ($R = 0.99$; RMSE = 0.86 m). The water volume fluctuates between -0.3 and 0.4 km³ month^{-1}, demonstrating strong agreement with in situ measurements ($R = 0.95$; RMSE = 0.0682 km³ month^{-1}). The study emphasizes the efficacy of diverse satellite observations for monitoring lake water storage variations, particularly beneficial for regions lacking in situ measurements or facing accessibility constraints (Pham-Duc et al., 2022).

In this study, Sentinel-3 SRAL (Synthetic Aperture Radar Altimeter) altimetry data will be employed to monitor variations in the water level in the Doroudzan dam reservoir. Consequently, an attempt is made to re-track the returned waveforms of the SRAL mission using the threshold re-tracking algorithm. Ultimately, the water level time series is selected with greater accuracy than in-situ gauges and is utilized to estimate the volume variations of the dam reservoir.

Furthermore, optical satellite images from the Sentinel-2 mission, characterized by excellent spatial and temporal resolution, are utilized to generate a time series depicting changes in the water surface area of the Doroudzan dam reservoir. By possessing information on both the water level and the water surface area of the dam reservoir, an estimation of the variations in the dam volume is presented and subsequently compared with in-situ volume data.

Additionally, a two-by-two analysis is conducted on changes in water level, water surface area, and dam reservoir volume, accompanied by identifying the most significant increases, decreases, and average changes in these parameters.

2. METHODS

2.1 Water level from L1B and L2 data from Sentinel-3A

Sentinel-3 constitutes an ocean and land mission, employing a constellation of two satellites, namely Sentinel-3A and Sentinel-3B. Sentinel-3A was launched on 16 February 2016, and its data became available in June 2016. Subsequently, Sentinel-3B was found on 25 April 2018, and its data became accessible from December 2018. This study utilized three years of Sentinel-3A data from March 2016 to December 2019. The SRAL instrument, serving as the primary topographic sensor for water level measurements, played a crucial role in our research and is detailed in (Q. Gao et al., 2019). To obtain altimeter measurements, Sentinel-3 SRAL transmits pulses at a Ku-band frequency, supplemented by a C-band frequency, to rectify range delay errors resulting from the varying electron density in

the ionosphere (Q. Gao et al., 2019). Sentinel-3 operates in two main modes: SAR mode and LRM. Given the global availability of SAR mode, we could retrieve inland water levels over any area tracked by Sentinel-3. Three levels of processed altimeter data are accessible: Level-0, Level-1, and Level-2 products. Our study used Level-1 non-time-critical (NTC) 20 Hz data to perform water level retrieval through the threshold re-tracking algorithm. Additionally, Sentinel-3 Level-2 re-trackers data from the European Space Agency (ESA) were employed for comparison. The primary objectives of Level-2 processing for SAR mode data are to furnish fundamental re-tracked altimeter estimates for various surfaces, including oceans, coastal zones, ice sheets, and sea ice elevations (Q. Gao et al., 2019; Tayfehrostami et al., 2022). Distinct re-tracking algorithms are better suited for specific surfaces in Level-2 data, such as ocean re-tracking, OCOG re-tracking, ice sheet re-tracking, ice re-tracking, and sea ice re-tracking. Regrettably, re-tracker results of ice-related surfaces are unavailable for inland water bodies. Consequently, we employed results from other Sentinel-3 Level-2 re-trackers for comparison.

The selected case study is Doroudzan Dam, situated at latitude 30°12'28" and longitude 52°25'5", located 70 km northwest of Shiraz-Marvdasht in Iran. Built on the Kor River, the dam regulates approximately 760 million cubic meters of water annually, primarily for irrigation in agricultural activities. The dam supports around 42 thousand hectares of land in the Ramjard block and approximately 34 thousand hectares in the Karbal and Kanara Marvdasht areas. Additionally, the power plant associated with this dam generates 45.5 gigawatt-hours of electricity each year. Through the examination of passes from the Sentinel-3A mission, it was observed that crossing number 253 provides substantial coverage of the study area.

A space-borne radar altimeter serves as a primary tool for monitoring oceans, and its applicability extends to inland water bodies, such as lakes, dams, and rivers. The principle of altimetry, as described in (Roohi, 2017), involves applying geophysical and atmospheric corrections. This study initially extracted altimetry data for 253 passes of the Sentinel-3A mission over the study area. Subsequently, corrections were implemented for the wet troposphere, dry troposphere, ionosphere, solid earth tide, geocentric pole tide, center of gravity (COG), and the geoid. Given that the study aimed to utilize official Sentinel-3A L1B data directly and compare it against Level-2 official products, the incorporation of corrections available in the Level-2 product was considered.

The threshold re-tracker, developed in 1997 primarily for measuring the height of ice sheets (Davis, 1997), offers key advantages, including implementation simplicity and internal accuracy in terms of repeatability (Davis, 1995). Here, repeatability refers to the stability of re-tracking in selecting the re-tracking point (Davis, 1997). The threshold re-tracker is typically assessed with 10%, 20%, and 50% thresholds. Research has shown that the 10% threshold yields the highest repeatability, while the 20% threshold is suitable for measurements over ice sheets. To determine the re-tracking gate, a linear interpolation is conducted between adjacent samples at a position where the threshold value intersects the leading edge of the waveform. The computational procedure is outlined as follows.

1. Thermal noise (PN) is obtained by averaging the first five gates:

$$P_N = \frac{1}{5}\sum_{i=1}^{5} P_i \quad , \qquad (1)$$

2. The amplitude is then calculated from the following Equation:

$$A = \sqrt{\frac{\sum_{i=1+n_1}^{N-n_2} iP_i^4(t)}{\sum_{i=1+n_1}^{N-n_2} P_i^2(t)}}, \qquad (2)$$

where N is the total number of waveform gates, and $n_1 = n_2 = 4$ are the beginning and end gates of waveform removed to prevent signal interference error (aliasing).

3. The threshold level is obtained from the following Equation:

$$Th = P_N + q(A - P_N) \quad , \qquad (3)$$

where A is calculated from Equation (2) and q is the threshold value (for example, 0.2 equals 20%).

4. The $Gate_{ret}$ is calculated from the following Equation:

$$Gate_{ret} = (k-1) + \frac{Th - P_{k-1}}{P_k - P_{k-1}}. \qquad (4)$$

where k is the first gate whose power exceeds the threshold Th. Figure (1) shows the re-tracked waveform of the 126th pass and 46th cycle using the threshold re-tracker for 10% to 90% thresholds.

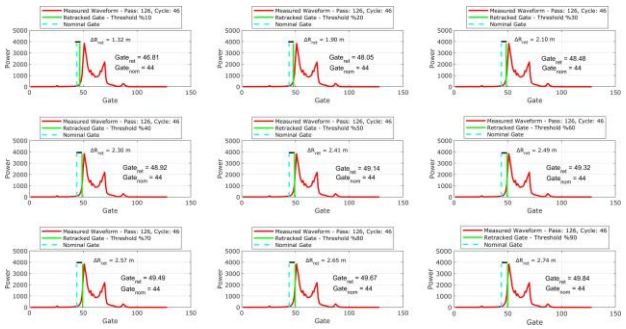

Figure 1. Re-tracking of the waveform for the 126th pass and the 46th cycle was conducted using the threshold algorithm with various thresholds.

2.2 Water surface area from Sentinel-2

In this study, we employed the Level-1C data from the Sentinel-2 mission imagery, selecting images with a cloudiness percentage below two percent based on the time series of altimetry data from the Sentinel-3A mission (one image per month). Sentinel-2 mission images are accessible online at (https://earthexplorer.usgs.gov/).

Water indices are commonly computed to improve the differentiation between water bodies and other objects. These indices are valued for their straightforward implementation and robust calculation capabilities, making them extensively utilized in dynamic analyses (Campos et al., 2012; Li & Roy, 2017; Tayfehrostami et al., 2023). The GEE-based monitoring in this study incorporates NDWI, thresholding, and post-processing techniques, including vegetation masking to eliminate non-water fields and minimum connection pixels to reduce sparse noise. The NDWI index is calculated as follows (B. C. Gao, 1996):

$$\mathrm{NDWI} = \frac{\rho_{Green} - \rho_{NIR}}{\rho_{Green} + \rho_{NIR}} \qquad (5)$$

Where ρ_{Green} and ρ_{NIR} are surface reflectance values of Sentinel-2 green and near-infrared bands, respectively. After applying the NDWI index to the images, Binary segmentation was conducted to extract water pixels from images. Ultimately, the water surface area of the study area was computed. Figure

(2) displays the Doroudzan dam reservoir extracted for November 6, 2019.

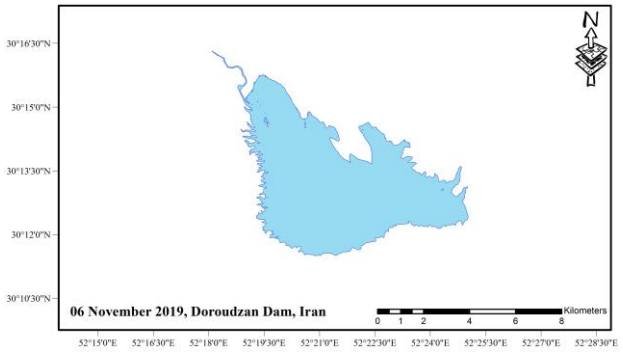

Figure 2. Extracted Dam Reservoir from Sentinel-2 Mission Images

2.3 Estimation of volume variations

With information on the water level and surface area of the dams' reservoirs, it becomes feasible to estimate the volume variations of the reservoirs by applying the Heron relation, as proposed by:

$$\Delta V = \frac{1}{3}(H_2 - H_1)\left(A_1 + A_2 + \sqrt{A_1 + A_2}\right) \quad (6)$$

In the equation provided above, ΔV represents the volume variations of the dam reservoir, while H1, H2, A1, and A2 denote the water levels and surface areas on adjacent dates, respectively.

Applying equation (6), the consecutive monthly volume variations of the dam reservoir were computed. Subsequently, by iteratively differentiating the time series of in-situ data for the absolute volume of the dam reservoir, monthly time series of volume variations were generated. The estimated volume variations time series were compared and evaluated using the correlation coefficient parameter against the time series of in-situ volume variations. The time series of water level changes and monthly water surface area changes were also calculated. A pairwise correlation analysis of these parameters and their average, maximum increase, and maximum decrease was also conducted.

Also, to validate and compare the estimated water level, water surface area, and volume variations obtained from the aforementioned missions, data from the Doroudzan Dam, sourced from the Iran Water Resources Management Company (https://www.wrm.ir/), were employed. This company releases comprehensive information in the periodic report on the hydrological and meteorological conditions of Iran's dams. The report comprises daily values for parameters including rainfall, evaporation, inflow, water level, reservoir volume, dam reservoir water surface area, and average temperature.

Furthermore, in the current study, the correlation coefficient (CORR) has been employed as an indicator to assess the extent of the direct (linear) relationship between the obtained results and the validation data. The relationship is articulated as follows (B. Wang, 2019):

$$\text{Corr} = \frac{\sum_{i=1}^{n}(A_i - \overline{A})(B_i - \overline{B})}{\sqrt{\sum_{i=1}^{n}(A_i - \overline{A})^2 \sum_{i=1}^{n}(B_i - \overline{B})^2}}. \quad (7)$$

Similarly, the root mean square index (RMSE) has been utilized in this study as a metric to assess the accuracy of the results. The relationship for the RMSE index is expressed as follows (B. Wang, 2019):

$$RMSE = \sqrt{\frac{\sum_{i=1}^{n}(A_i - B_i)^2}{n}} \quad (8)$$

In the relationships above, A_i represents the estimated results, $\overline{A}$ is their average, B_i denotes the validation data, $\overline{B}$ is its average, and n represents the amount of data. The correlation coefficient assumes values between -1 and +1; a value closer to one signifies a stronger direct correlation between the two data series. This parameter's sign indicates the connection's nature, whether direct or inverse. Furthermore, a smaller RMSE value is indicative of better accuracy. The relation of the relative RMSE index is as follows:

$$RRMSE = \frac{RMSE}{\overline{A}} \times 100\% \quad (9)$$

3. RESULTS

Initially, to monitor the water level of Doroudzan Dam, an analysis of Level-2 and Level-1B SAR altimetry data from the Sentinel-3A mission was conducted. The time series of the water level was obtained, and results indicated that the OCOG re-tracker yielded results closer to the in-situ gauge than other re-trackers in the Level-2 data.

Furthermore, re-tracking the returned waveforms using the threshold algorithm revealed that the water level time series calculated with a 60% threshold provided superior results compared to other thresholds and closely matched the in-situ gauge measurements. Subsequently, the time series of the optimal water level for Doroudzan Dam, obtained from processing Level-2 data and re-tracking the returned waveforms with a 60% threshold, were consolidated. The outcomes are presented in Table 1, which was then compared with in-situ gauge measurements using parameters such as Root Mean Square Error (RMSE), correlation coefficient.

Table 1. Evaluation of the final time series of the water level of Doroudzan Dam.

Method	RMSE (cm)	CORR (%)
L2 processing - OCOG	38.23	99.23
60% threshold	37.73	99.30

The findings in Table 1 demonstrate that re-tracking the returned waveforms with the threshold algorithm, explicitly using a 60% threshold, enhances accuracy by 1.3%. Additionally, it exhibits a 0.07% higher correlation with the in-situ gauge than the water level obtained from the OCOG re-tracker. Figure (3) illustrates the conclusive time series of water levels for Doroudzan Dam based on these improved results.

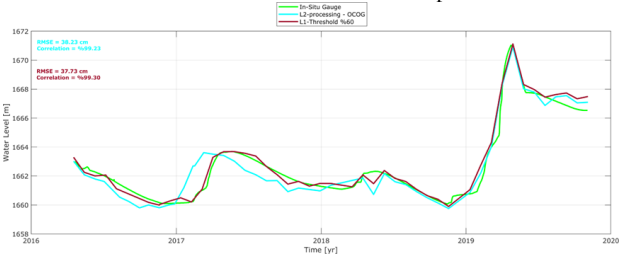

Figure 3. The final time series of the water level of Doroudzan Dam.

Following the pre-processing and post-processing steps detailed in section 3.2, the time series of the water surface area was extracted from Sentinel-2 mission images. This extracted time series of the water surface area from Sentinel-2 images was then compared with the in-situ surface area time series, utilizing two

parameters: correlation coefficient and relative RMSE, as depicted in Figure (4).

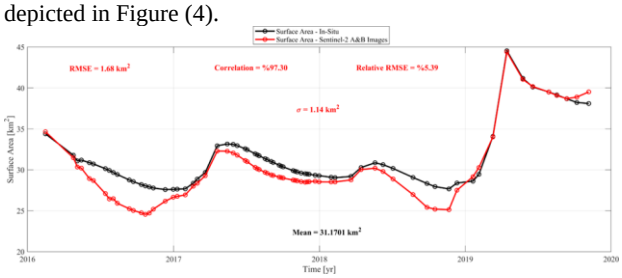

Figure 4. Time series of surface areas obtained from Sentinel-2 and in-situ data.

The evaluation and comparison of the two time series yielded relative RMSE values of 5.39% and a correlation of 97.30%. These results demonstrate the excellent and effective performance of the method employed for calculating the water surface area of Doroudzan Dam from the optical images of the Sentinel-2 mission.

Finally, the successive volume variations of the dam reservoir were calculated by inputting the time series of water level and surface area into Heron's relation. Figure (5) showed the estimated subsequent volume variations of the Doroudzan Dam reservoir.

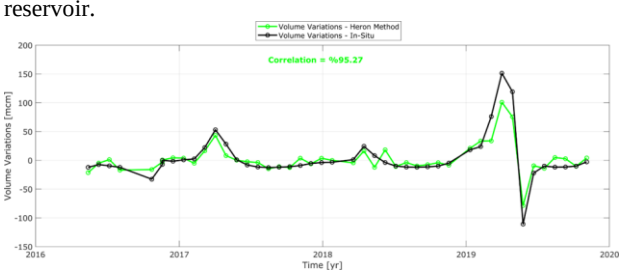

Figure 5. Time series of volume variations from Heron's relation and in-situ data.

The estimated time series of volume variations exhibited a high correlation of 95.27% with the in-situ volume variation time series. This high correlation underscores the optimal utilization of input parameters for Heron's equation, namely water level and surface area, and the enhanced capability of this equation to calculate volume variations accurately.

The analysis results for the highest increase, highest decrease, and average variations of three parameters—water level, surface area, and volume of Doroudzan Dam—are presented in Table 2.

Table 2. The greatest increase, the greatest decrease, and the average variations in the water level, surface area, and water volume.

Parameter	Water level variations (m)	surface area variations (km^2)	Volume variations (mcm)
Average	0.09	0.17	2.33
Highest increase	4.09	7.07	100.94
Highest decrease	-2.80	-2.22	-78.61

According to Table 2, the highest increase in water level, surface area, and volume occurred with values of 4.09 meters, 7.07 km^2, and 100.94 million cubic meters (mcm) from March 6, 2019, to April 2, 2019. This period typically experiences increased rainfall. Conversely, the most significant decrease in water level, surface area, and volume was observed from April 29, 2019, to May 26, 2019, with values of 2.80 meters, 2.22 km^2, and 78.61 mcm, respectively.

Additionally, Table 2 reveals the average water level, surface area, and volume increase over the entire study period.

The correlation analysis conducted for the three parameters—water level, surface area, and volume variations—revealed a correlation of 98.86% between water level and volume variations, 84.97% between water surface area and volume variations, and 87.23% between water level and water surface area variations. These results indicate a robust linear correlation among the three time series of variations in water level, surface area, and volume. Figure (6) visually presents the analysis results described in this section.

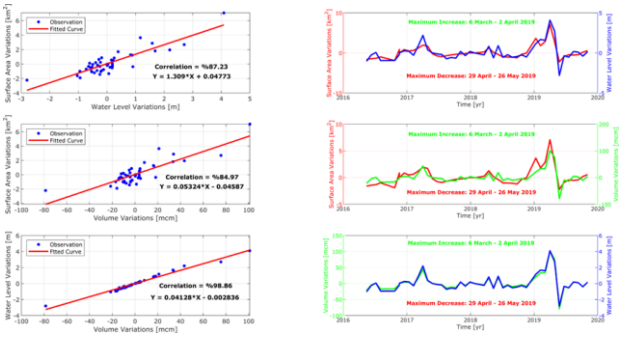

Figure 6. Correlation analysis between variations in water level, surface area, and volume.

4. DISCUSSION&CONCLUSION

In this study, variations in water level, surface area, and volume of the Doroudzan Dam reservoir in Iran were investigated utilizing different missions of Copernicus satellites. The Sentinel-3A altimetry mission, the first to capture the entire globe in SAR mode with a footprint size of 300 meters along the track, was employed to monitor water levels. Additionally, Sentinel-2 mission images were utilized to monitor the water surface area of the dam reservoir concurrently with altimetry data. By inputting the water level and water surface area information into Heron's equation, the time series of volume variations for the dam reservoir were derived. The summarized results are as follows:

1) The re-tracking of returned waveforms with the threshold algorithm using a 60% threshold improves accuracy by 1.3% and increases the correlation by 0.07% compared to the water level time series obtained from the OCOG re-tracker of Level-2 (L2) data in comparison with the in-situ gauge.

2) The evaluation and comparison of the time series of estimated surface areas from Sentinel-2 satellite imagery and in-situ surface areas resulted in relative RMSE values of 5.39% and a correlation of 97.30%. These outcomes underscore the excellent and effective performance of the method employed for calculating the water surface area of Doroudzan Dam using optical images from the Sentinel-2 mission.

3) The analysis conducted for the correlation between the three parameters of variations in water level, surface area, and volume revealed a 98.86% correlation between variations in water level and volume, 84.97% between variations in surface area and volume, and 87.23% between variations in water level and water surface area.

4) The highest increase in water level, surface area, and water volume occurred with values of 4.09 meters, 7.07 km^2, and 100.94 mcm from March 6, 2019, to April 2, 2019, which typically experiences higher rainfall. Conversely, the most significant decrease in water level, surface area, and volume variations occurred from April 29, 2019, to May 26, 2019, with values of 2.80 meters, 2.22 km^2, and 78.61 mcm, respectively. Furthermore, the results indicate an average increase in the water level, surface area, and volume of Doroudzan Dam during the study period.

The results of this study highlight the high capability and effective performance of various missions from Copernicus satellites in monitoring inland water bodies. Additionally, the study underscores the effectiveness of the methods employed to monitor volume variations in dam reservoirs.

ACKNOWLEDGEMENTS

The authors would like to express their gratitude and thank the Iran Water Resources Management Company for providing the essential in-situ data and information required for the Doroudzan Dam. Additionally, we are thankful to the European Space Agency (ESA) and the European Organization for the Exploitation of Meteorological Satellites (EUMETSAT) for supplying the satellite mission data utilized in this study.

REFERENCES

Ahmadi, A., Jalali, J., & Mohammadpour, A. (2022). Future runoff assessment under climate change and land-cover alteration scenarios: a case study of the Zayandeh-Roud dam upstream watershed. *Hydrology Research*, *53*(11), 1372–1392. https://doi.org/10.2166/nh.2022.056

Barezaei, A., & Jalali, J. (2023). a Comparison of Simulated Runoff Based on Ground Rain Gauges and Persiann-Cdr Satellite Precipitation Records Using Swat Model. *ISPRS Annals of the Photogrammetry, Remote Sensing and Spatial Information Sciences*, *10*(4/W1-2022), 87–94. https://doi.org/10.5194/isprs-annals-X-4-W1-2022-87-2023

Biancamaria, S., Frappart, F., Leleu, A. S., Marieu, V., Blumstein, D., Desjonquères, J. D., Boy, F., Sottolichio, A., & Valle-Levinson, A. (2017). Satellite radar altimetry water elevations performance over a 200 m wide river: Evaluation over the Garonne River. *Advances in Space Research*, *59*(1), 128–146. https://doi.org/10.1016/j.asr.2016.10.008

Birkett, C. M. (1995). The contribution of TOPEX/POSEIDON to the global monitoring of climatically sensitive lakes. *Journal of Geophysical Research*, *100*(C12), 25179. https://doi.org/10.1029/95JC02125

Birkinshaw, S. J., O'Donnell, G. M., Moore, P., Kilsby, C. G., Fowler, H. J., & Berry, P. A. M. (2010). Using satellite altimetry data to augment flow estimation techniques on the Mekong River. *Hydrological Processes*, *24*(26), 3811–3825. https://doi.org/10.1002/hyp.7811

Campos, J. C., Sillero, N., & Brito, J. C. (2012). Normalized difference water indexes have dissimilar performances in detecting seasonal and permanent water in the Sahara-Sahel transition zone. *Journal of Hydrology*, *464–465*(464–465), 438–446. https://doi.org/10.1016/j.jhydrol.2012.07.042

Cazenave, A., Bonnefond, P., Dominh, K., & Schaeffer, P. (1997). Caspian sea level from Topex-Poseidon altimetry: Level now falling. *Geophysical Research Letters*, *24*(8), 881–884. https://doi.org/10.1029/97GL00809

Crétaux, J.-F., Kouraev, A. V, Papa, F., Nguyen, M. B., Cazenave, A., Aladin, N. V, & Plotnikov, I. S. (2005). Evolution of Sea Level of the Big Aral Sea from Satellite Altimetry and Its Implications for Water Balance. *Journal of Great Lakes Research*, *31*(4). https://doi.org/10.1016/S0380-1330(05)70281-1ï

Crétaux, J. F., Abarca-del-Río, R., Bergé-Nguyen, M., Arsen, A., Drolon, V., Clos, G., & Maisongrande, P. (2016). Lake Volume Monitoring from Space. In *Surveys in Geophysics* (Vol. 37, Issue 2, pp. 269–305). Springer Netherlands. https://doi.org/10.1007/s10712-016-9362-6

Davis, C. H. (1995). Growth of the Greenland Ice Sheet: A Performance Assessment of Altimeter Retracking Algorithms. *IEEE Transactions on Geoscience and Remote Sensing*, *33*(5), 1108–1116. https://doi.org/10.1109/36.469474

Davis, C. H. (1997). A robust threshold retracking algorithm for measuring ice-sheet surface elevation change from satellite radar altimeters. *IEEE Transactions on Geoscience and Remote Sensing*, *35*(4), 974–979. https://doi.org/10.1109/36.602540

Domeneghetti, A., Tarpanelli, A., Brocca, L., Barbetta, S., Moramarco, T., Castellarin, A., & Brath, A. (2014). The use of remote sensing-derived water surface data for hydraulic model calibration. *Remote Sensing of Environment*, *149*, 130–141. https://doi.org/10.1016/j.rse.2014.04.007

Duan, Z., & Bastiaanssen, W. G. M. (2013). Estimating water volume variations in lakes and reservoirs from four operational satellite altimetry databases and satellite imagery data. *Remote Sensing of Environment*, *134*, 403—416. https://doi.org/10.1016/j.rse.2013.03.010

Eakins, B. W., & Sharman, G. F. (2010). Volumes of the World's Oceans from ETOPO1. *NOAA National Geophysical Data Center, Boulder, CO*, *7*, 1.

Frappart, F., Calmant, S., Cauhopé, M., Seyler, F., & Cazenave, A. (2006). Preliminary results of ENVISAT RA-2-derived water levels validation over the Amazon basin. *Remote Sensing of Environment*, *100*(2), 252–264. https://doi.org/10.1016/j.rse.2005.10.027

Frappart, F., Do Minh, K., L'Hermitte, J., Cazenave, A., Ramillien, G., Le Toan, T., & Mognard-Campbell, N. (2006). Water volume change in the lower Mekong from satellite altimetry and imagery data. *Geophysical Journal International*, *167*(2), 570–584. https://doi.org/10.1111/j.1365-246X.2006.03184.x

Frappart, F., Papa, F., Famiglietti, J. S., Prigent, C., Rossow, W. B., & Seyler, F. (2008). Interannual variations of river water storage from a multiple satellite approach: A case study for the Rio Negro River basin. *Journal of Geophysical Research Atmospheres*, *113*(21). https://doi.org/10.1029/2007JD009438

Frappart, F., Papa, F., Güntner, A., Werth, S., Ramillien, G., Prigent, C., Rossow, W. B., & Bonnet, M. P. (2010). Interannual variations of the terrestrial water storage in the lower ob' basin from a multisatellite approach. *Hydrology and Earth System Sciences*, *14*(12), 2443–2453. https://doi.org/10.5194/hess-14-2443-2010

Frappart, F., Papa, F., Güntner, A., Werth, S., Santos da Silva, J., Tomasella, J., Seyler, F., Prigent, C., Rossow, W. B., Calmant, S., & Bonnet, M. P. (2011). Satellite-based estimates of groundwater storage variations in large drainage basins with extensive floodplains. *Remote Sensing of Environment*, *115*(6), 1588–1594. https://doi.org/10.1016/j.rse.2011.02.003

Frappart, F., Seyler, F., Martinez, J. M., León, J. G., & Cazenave, A. (2005). Floodplain water storage in the Negro River basin estimated from microwave remote sensing of inundation area and water levels. *Remote Sensing of Environment*, *99*(4), 387–399. https://doi.org/10.1016/j.rse.2005.08.016

Gao, B. C. (1996). NDWI - A normalized difference water index for remote sensing of vegetation liquid water from space. *Remote Sensing of Environment*, *58*(3), 257–266. https://doi.org/10.1016/S0034-4257(96)00067-3

Gao, Q., Makhoul, E., Escorihuela, M. J., Zribi, M., Seguí, P. Q., García, P., & Roca, M. (2019). Analysis of retrackers' performances and water level retrieval over the Ebro River basin using sentinel-3. *Remote Sensing*,

11(6), 718. https://doi.org/10.3390/RS11060718

Gleick, P. (Oxford university). (19993). Water in Crisis Book.pdf. *Ibiologia.Unam.Mx*. http://www.ibiologia.unam.mx/pdf/directorio/z/introduccion/world_watershed_re.pdf

He, F., Mohamadzadeh, N., Sadeghnejad, M., Ingram, B., & Ostovari, Y. (2023). Fractal Features of Soil Particles as an Index of Land Degradation under Different Land-Use Patterns and Slope-Aspects. *Land*, *12*(3). https://doi.org/10.3390/land12030615

Jalali, J., Ahmadi, A., & Abbaspour, K. (2021). Runoff responses to human activities and climate change in an arid watershed of central Iran. *Hydrological Sciences Journal*, *66*(16), 2280–2297. https://doi.org/10.1080/02626667.2021.1985724

Kim, Y., Schmid, T., Charbiwala, Z. M., Friedman, J., & Srivastava, M. B. (2008). NAWMS: Nonintrusive autonomous water monitoring system. *SenSys'08 - Proceedings of the 6th ACM Conference on Embedded Networked Sensor Systems*, 309–321. https://doi.org/10.1145/1460412.1460443

Kordi, F., & Yousefi, H. (2022). Crop classification based on phenology information by using time series of optical and synthetic-aperture radar images. *Remote Sensing Applications: Society and Environment*, *27*, 100812. https://doi.org/10.1016/j.rsase.2022.100812

Kouraev, A. V., Zakharova, E. A., Samain, O., Mognard, N. M., & Cazenave, A. (2004). Ob' river discharge from TOPEX/Poseidon satellite altimetry (1992-2002). *Remote Sensing of Environment*, *93*(1–2), 238–245. https://doi.org/10.1016/j.rse.2004.07.007

Leon, J. G., Calmant, S., Seyler, F., Bonnet, M. P., Cauhopé, M., Frappart, F., Filizola, N., & Fraizy, P. (2006). Rating curves and estimation of average water depth at the upper Negro River based on satellite altimeter data and modeled discharges. *Journal of Hydrology*, *328*(3–4), 481–496. https://doi.org/10.1016/j.jhydrol.2005.12.006

Li, J., & Roy, D. P. (2017). A global analysis of Sentinel-2a, Sentinel-2b and Landsat-8 data revisit intervals and implications for terrestrial monitoring. *Remote Sensing*, *9*(9), 902. https://doi.org/10.3390/rs9090902

Lin, Y., Li, X., Zhang, T., Chao, N., Yu, J., Cai, J., & Sneeuw, N. (2020). Water volume variations estimation and analysis using multisource satellite data: A case study of Lake Victoria. *Remote Sensing*, *12*(18). https://doi.org/10.3390/RS12183052

Liu, C., Hu, R., Wang, Y., Lin, H., Zeng, H., Wu, D., Liu, Z., Dai, Y., Song, X., & Shao, C. (2022). Monitoring water level and volume changes of lakes and reservoirs in the Yellow River Basin using ICESat-2 laser altimetry and Google Earth Engine. *Journal of Hydro-Environment Research*, *44*, 53–64. https://doi.org/10.1016/j.jher.2022.07.005

Medina, C., Gomez-Enri, J., Alonso, J. J., & Villares, P. (2010). Water volume variations in Lake Izabal (Guatemala) from in situ measurements and ENVISAT Radar Altimeter (RA-2) and Advanced Synthetic Aperture Radar (ASAR) data products. *Journal of Hydrology*, *382*(1–4), 34–48. https://doi.org/10.1016/j.jhydrol.2009.12.016

Mercier, F., Cazenave, A., Change, C. M.-G. and P., & 2002, undefined. (n.d.). Interannual lake level fluctuations (1993–1999) in Africa from Topex/Poseidon: connections with ocean–atmosphere interactions over the Indian Ocean. *Elsevier*. Retrieved May 8, 2021, from https://www.sciencedirect.com/science/article/pii/S0921818101001394

Mohammadpouri, S., Sadeghnejad, M., Rezaei, H., Ghanbari, R., Tayebi, S., Mohammadzadeh, N., Mijani, N., Raeisi, A., Fatholoumi, S., & Biswas, A. (2023). A Generalized Regression Neural Network Model for Accuracy Improvement of Global Precipitation Products: A Climate Zone-Based Local Optimization. *Sustainability*, *15*(11). https://doi.org/10.3390/su15118740

Morris, C. S., & Gill, S. K. (1994). Variation of Great Lakes water levels derived from Geosat altimetry. *Water Resources Research*, *30*(4), 1009–1017. https://doi.org/10.1029/94WR00064

Nilsson, C. (2009). Reservoirs. In G. E. Likens (Ed.), *Encyclopedia of Inland Waters* (pp. 625–633). Academic Press. https://doi.org/10.1016/B978-012370626-3.00039-9

Peng, D., Guo, S., Liu, P., & Liu, T. (2006). Reservoir Storage Curve Estimation Based on Remote Sensing Data. *Journal of Hydrologic Engineering*, *11*(2), 165–172. https://doi.org/10.1061/(asce)1084-0699(2006)11:2(165)

Pham-Duc, B., Frappart, F., Tran-Anh, Q., Si, S. T., Phan, H., Quoc, S. N., Le, A. P., & Viet, B. Do. (2022). Monitoring Lake Volume Variation from Space Using Satellite Observations—A Case Study in Thac Mo Reservoir (Vietnam). *Remote Sensing*, *14*(16). https://doi.org/10.3390/rs14164023

Roohi, S. (2017). Performance evaluation of different satellite radar altimetry missions for monitoring inland water bodies. *Geodätisches Institut Der Universität Stuttgart*, *March*, 173.

Santos da Silva, J., Calmant, S., Seyler, F., Rotunno Filho, O. C., Cochonneau, G., & Mansur, W. J. (2010). Water levels in the Amazon basin derived from the ERS 2 and ENVISAT radar altimetry missions. *Remote Sensing of Environment*, *114*(10), 2160–2181. https://doi.org/10.1016/j.rse.2010.04.020

Schneider, R., Tarpanelli, A., Nielsen, K., Madsen, H., & Bauer-Gottwein, P. (2018). Evaluation of multi-mode CryoSat-2 altimetry data over the Po River against in situ data and a hydrodynamic model. *Advances in Water Resources*, *112*, 17–26. https://doi.org/10.1016/j.advwatres.2017.11.027

Singh, A., Seitz, F., & Schwatke, C. (2012). Inter-annual water storage changes in the Aral Sea from multi-mission satellite altimetry, optical remote sensing, and GRACE satellite gravimetry. *Remote Sensing of Environment*, *123*, 187–195. https://doi.org/10.1016/j.rse.2012.01.001

Smith, L. C., & Pavelsky, T. M. (2009). Remote sensing of volumetric storage changes in lakes. *Earth Surface Processes and Landforms*, *34*(10), 1353–1358. https://doi.org/10.1002/esp.1822

Sulistioadi, Y. B., Tseng, K.-H., Shum, C. K., Hidayat, H., Sumaryono, M., Suhardiman, A., Setiawan, F., & Sunarso, S. (2015). Satellite radar altimetry for monitoring small rivers and lakes in Indonesia. *Hydrol. Earth Syst. Sci*, *19*, 341–359. https://doi.org/10.5194/hess-19-341-2015

Tarpanelli, A., Barbetta, S., Brocca, L., & Moramarco, T. (2013). River Discharge Estimation by Using Altimetry Data and Simplified Flood Routing Modeling. *Remote Sensing*, *5*(9), 4145–4162. https://doi.org/10.3390/rs5094145

Tarpanelli, A., & Benveniste, J. (2019). On the potential of altimetry and optical sensors for monitoring and forecasting river discharge and extreme flood events. In *Extreme Hydroclimatic Events and Multivariate Hazards in a Changing Environment* (pp. 267–287). Elsevier.

https://doi.org/10.1016/b978-0-12-814899-0.00011-0

Tayfehrostami, A., Abedini, A., & Tajfirooz, B. (2023). Analyzing the variations in the water surface area of Taleqan Dam of Iran using ground-based and satellite observations. *2023 International Conference on Machine Intelligence for GeoAnalytics and Remote Sensing, MIGARS 2023*, *1*, 1–4. https://doi.org/10.1109/MIGARS57353.2023.10064509

Tayfehrostami, A., Ardalan, A. A., & Pourmina, A. H. (2022). River discharge monitoring using satellite missions : Sentinel - 1 , Sentinel - 2 , and Sentinel - 3 (Case study : The Karun River , Iran). *Earth Observation and Geomatics Engineering*, *5*(2), 96–111.

Tong, X., Pan, H., Xie, H., Xu, X., Li, F., Chen, L., Luo, X., Liu, S., Chen, P., & Jin, Y. (2016). Estimating water volume variations in Lake Victoria over the past 22 years using multi-mission altimetry and remotely sensed images. *Remote Sensing of Environment*, *187*, 400–413. https://doi.org/10.1016/j.rse.2016.10.012

Wang, B. (2019). *Monitoring inland surface water level from Sentinel-3 data*. http://dx.doi.org/10.18419/opus-10285

Wang, W., Lu, H., Ruby Leung, L., Li, H.-Y., Zhao, J., Tian, F., Yang, K., & Sothea, K. (2017). Dam Construction in Lancang-Mekong River Basin Could Mitigate Future Flood Risk From Warming-Induced Intensified Rainfall. *Geophysical Research Letters*, *44*(20), 10,378-10,386. https://doi.org/10.1002/2017GL075037

Zarfl, C., Lumsdon, A. E., Berlekamp, J., Tydecks, L., & Tockner, K. (2015). A global boom in hydropower dam construction. *Aquatic Sciences*, *77*(1), 161–170. https://doi.org/10.1007/s00027-014-0377-0

Zhang, J., Xu, K., Yang, Y., Qi, L., Hayashi, S., & Watanabe, M. (2006). MEASURING WATER STORAGE FLUCTUATIONS IN LAKE DONGTING, CHINA, BY TOPEX/POSEIDON SATELLITE ALTIMETRY. *Environmental Monitoring and Assessment*, *115*(1–3), 23–37. https://doi.org/10.1007/s10661-006-5233-9

Zhou, T., Nijssen, B., Gao, H., & Lettenmaier, D. P. (2016). The contribution of reservoirs to global land surface water storage variations. *Journal of Hydrometeorology*, *17*(1), 309–325. https://doi.org/10.1175/JHM-D-15-0002.1